AAPG Datapages/Search and Discovery Article #90174 CSPG©2014 CSPG/CSEG/CWLS GeoConvention 2012, (Vision) May 14-18, 2012, Calgary, AB, Canada

Importance of Pre-Frack Site Surveys and Broadband Seismometers to Microseismic Monitoring

N. Ackerley, Nanometrics, Inc., Kanata, Canada
and
N. Spriggs, Nanometrics, Inc., Kanata, Canada
NeilSpriggs@nanometrics.ca

Summary

Site surveys using broadband seismometers at the surface and in shallow postholes have great utility to microseismic monitoring. Site noise can vary greatly from one location to another, because of proximity to sources of cultural noise, and because of subsurface geology. With a preliminary survey, sensors at the noisiest sites can be relocated to quieter sites before the operation to be monitored starts. Furthermore, accurate site noise estimates allow accurate estimation of minimum expected detectable events. Finally, accurate estimates of the inelastic attenuation in the area to be studied are essential for estimating event spectra.

The use of broadband sensors gives several specific benefits over traditional geophone instrumentation. It can be argued that the noise floor improvement from 2-100 Hz is more-or-less balanced by the noise-floor degradation above 100 Hz. Regardless of the outcome of this balancing, there are at least three significant advantages to broadband instrumentation. First, the ability to resolve the microseismic peak at 0.2 Hz means that relative misalignment of three-channel instrumentation can be computed and corrected across the array. Second, the low noise floor at 1 Hz allows the end-user to exploit the ubiquitous notch in site noise at that frequency. Third, broadband instrumentation makes it much easier to distinguish near-local events from regional events, and greatly reduces the risk of misinterpretation of data.

Introduction

Microseismic monitoring is a key technology in the emerging fields of hydraulic fracturing, geothermal power generation and carbon sequestration. In each case, fluids are pumped underground at high pressures, and the resulting ground motion can be detected and localized using seismic sensors. Typical depths for hydraulic fracturing in Barnett and Marcellus shale are 1-3 km (see Fisher, 2010). Basic microseismic analysis would aim to detect as many events as possible, locate and map them and estimate their magnitudes.

If events can be located routinely and quickly enough, then situations where the stimulated volume encroaches on a reservoir or a pre-existing fault can be detected and injection halted. With an exhaustive catalog of injection-induced events it becomes possible to, estimate probability and recurrence intervals of damaging events.

Down-hole sensor strings allow some events to be observed at closer range, and avoid excess site noise at the surface. However, it can be prohibitively expensive to have many such boreholes, and vertically-arrayed sensors constrain the horizontal location of an event relatively poorly.

Surface arrays should be less expensive to deploy and will give better estimates of horizontal locations of events. Since events generated tend to be located within the particular strata being stimulated the heights are already well constrained, so it is not a disadvantage that a surface array results in greater depth uncertainty. The problems with surface arrays are that hypocentral distances can be no smaller than the depth of the gas-bearing strata, and are more susceptible to cultural and other sources of surface noise.

The problem of detectability of small events can be addressed in terms of signal-to-noise ratios. The question is whether the signal to be measured is larger than the noise, and by how much.

Method

The ground motion due to an event depends on the source mechanism (e.g. slip, implosion or explosion), the hypocentral distance (i.e. the distance from the source to the receiver) the physical properties of the earth, particularly near the source and the receiver and the depth of the sensor. For a typical earthquake the source mechanism is slippage at a fault, and the dimensions of the slip plane and the position of the receiver with respect to the orientation of the slip plane also matter.

The noise which may obscure an event signal consists of the self-noise of the seismograph system and the site noise. The seismograph system consists of a sensor and a digitizer, each with their own self-noise .The self-noise of well-constructed digitizers and seismometers is stationary, (i.e. random and not time-dependent) and so well-represented by a power spectral density (PSD). For the purposes of this study, it will be assumed that digitizer can be configured to have a high enough gain that its noise contribution is negligible.

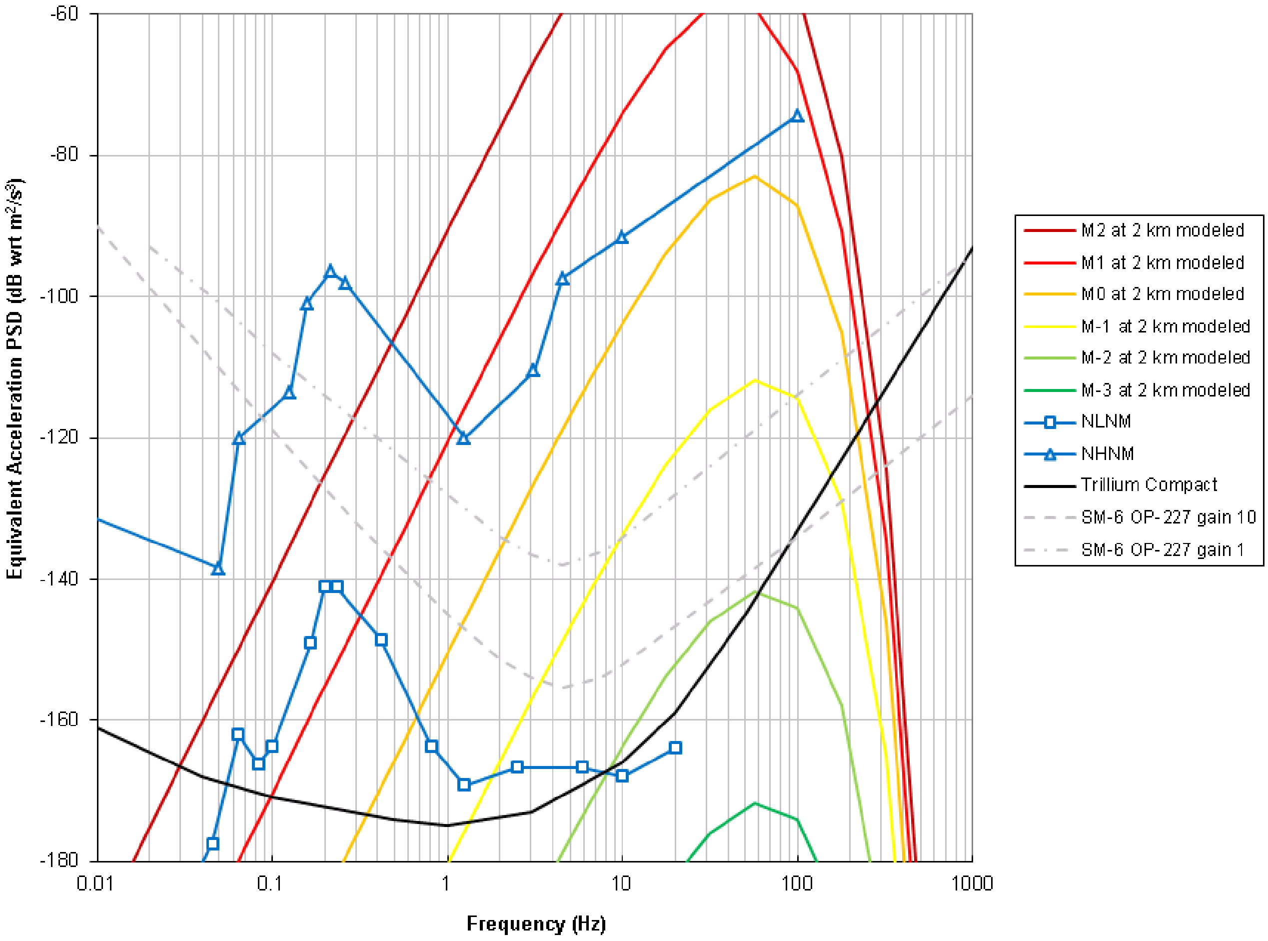

Figure 1: Estimating Signal-to-Noise Ratios for Very Small Events

The site noise will have some components which are stationary and some which are not. The noise will also be spatially correlated in some bands and not in others. To the extent that the signal is stationary, the PSD of one time period will be representative of every time period. Because it is not stationary, the PSD probability density function (PDF) is a useful way of visualizing the signal; rather than assigning a single value per frequency, one has a probability distribution at each frequency. This is very useful for visualizing bimodal PDFs due, for example to diurnal variations in background noise. The Nanometrics software tool SQLX is ideally suited for this type of task. To the extent that the noise is spatially correlated, the site noise can be reduced by array-processing methods, including, in some cases, simple stacking. In any case it is important to have a good understanding of the characteristics of site noise before attempting to detect events.

Because events are fundamentally transient signals, power spectral density is not a good measure of the power in a given bandwidth. However for the purposes of comparison to seismograph and site noise PSDs, if an equivalent bandwidth and a crest factor are assumed, then one can compute a comparable equivalent spectrum. Ackerley (2012) furthermore shows how the spectra of Brune (1970) can be reconciled to the measured event spectra of Clinton and Heaton, and scales these spectra down to very small magnitudes appropriate for microseismic monitoring.

Putting all of these notions together, Figure 1 summarizes the detectability problem for very small events.

The grey and black lines are sensor self-noise PSDs. The grey lines represent 4.5 Hz geophones with high- and low-gain preamplifiers; it is worth noting that the noise cannot be pushed much lower than this with increasing gain, only a geophone with higher-sensitivity and/or lower corner frequency will have lower self-noise. The black line is the self-noise of a broadband seismometer, the Nanometrics Trillium Compact. The geophone with the high-gain preamp has lower noise above about 100 Hz; below that frequency the seismometer is much quieter.

The red, yellow, orange and green lines are equivalent acceleration PSDs of Brune spectra computed according to Ackerley (2012). “Notwithstanding excess ground motion due to site noise, we can conclude that a Trillium Compact should be able to detect an M-2 event more than 50% of the time, but not an M-3 event at this range. A high-gain geophone will similarly be able to detect an M-2 event significantly less than 50% of the time, and a high-gain geophone will be able to detect M-1 events, but not M-2 events.“ Of course, this only applies at sites which are very quiet, such as those deep underground in competent bedrock at very remote locations.

The blue lines in Figure 1 are models of the noise observed at seismic observatories, compiled by Peterson (1993). The NLNM and NHNM are common reference points in seismology; they represent fictional quietest and noisiest possible good sites. (Of course a site can be even noisier if it is intentionally made bad, for example if you were to install your seismometer on a waterbed flying a flagpole.) Although just about any site will be within 10 dB of the NLNM at the microseismic peak (0.1 to 1 Hz), it can be quite difficult to find a site that quiet above 1 Hz. The NLNM and NHNM therefore bracket the range of possible noise levels which will be observed.

Clearly, at noisy sites it does not matter how quiet the sensor is; if the site is as noisy as the NHNM then you will not even be able to measure an M0 event with any sensor. This, then, is the main motivation for doing pre-injection site surveys. To the extent that the site noise is stationary, a preliminary survey can be used to determine the limits of detectability and properly design the array to be used to monitor the injection.

Note also that the high-frequency roll-off of event spectra is controlled by the intrinsic attenuation of the medium, characterised by the quality factor. For the event spectra shown in Figure 1 Q = 50 was used. This is another reason to do a pre-injection survey; if the local quality factor is greater or lesser then stimulated events will more or less high-frequency content, respectively.

Rolla Microseismic Experiment

The Rolla Microseismic Experiment was carried out by the Microseismic Industry Consortium in August of 2012. The objective of the experiment was to determine the utility of low-frequency seismic data.

Sensors were deployed in four mini-arrays of four three-component seismometers, labeled A-D in Figure 2, plus the addition of two single three-component seismometers, labeled E and F. The arrays formed a diamond shape, pointing at the injection well head. The sensor spacing was chosen to be 33 m, so that surface waves traveling at a velocity of 1000 m/s should cancel exactly at 15 Hz. Station locations were constrained to some extent by permissions, harvest times, etc.

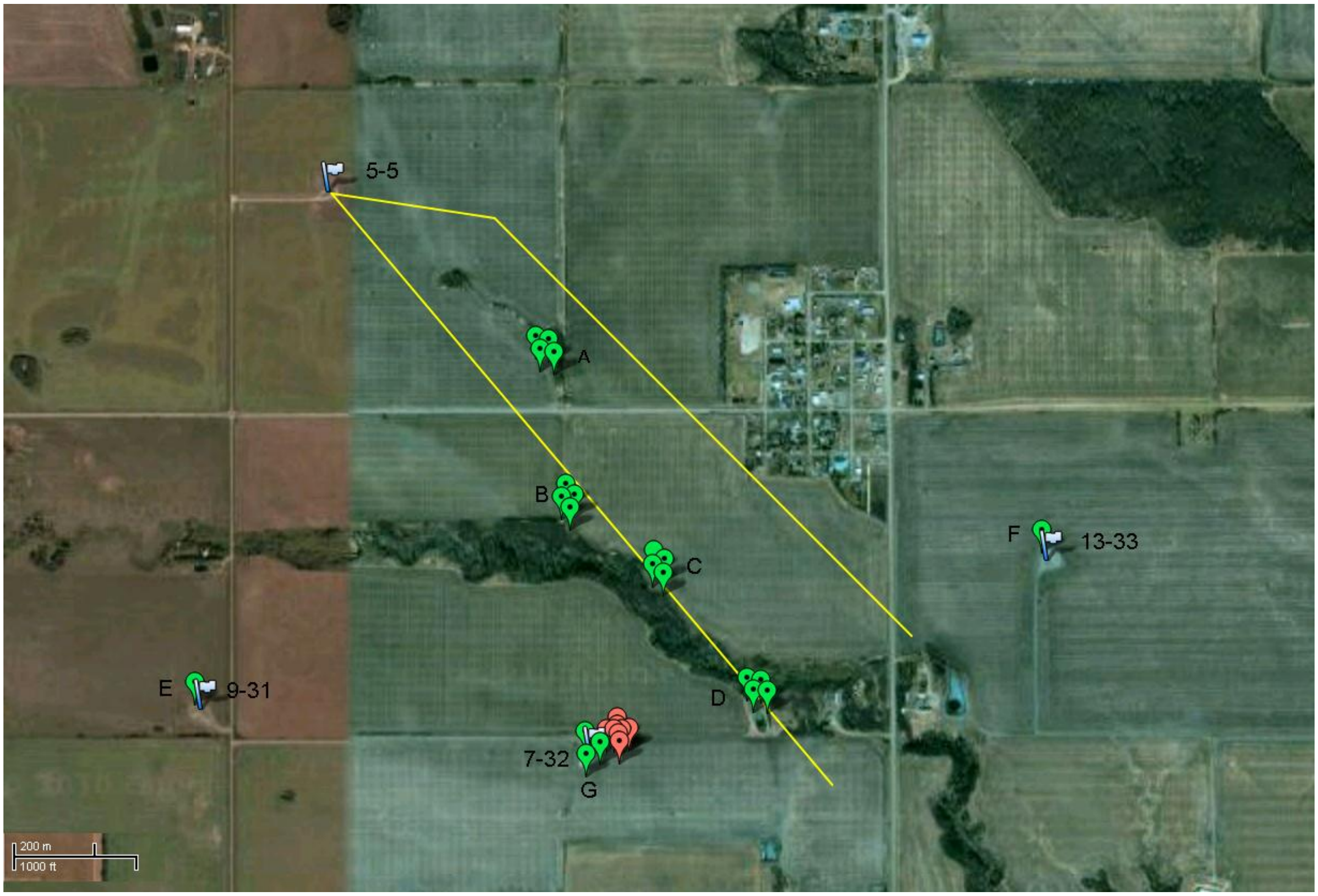

Figure 2: Rolla Microseismic Experiment Array Deployment

Sensors were installed in shallow postholes at approximately 1 m depth, i.e. an arm's reach, and aligned using a compass, as shown in Figure 3. Each sensor is sitting on a cradle with a spike driven approximately a foot into the soil. The standard Trillium Compact carrying case also serves as a cover so that soil is not piled directly onto the sensor. The Nanometrics Taurus digitizer and batteries were housed in a shallowly buried cooler nearby, and data timing was ensured using GPS.

Figure 3: Shallow Posthole Installation

The arrays were deployed from August 8-27, with continuous recording at 500 sps. Two horizontal wells were fractured in ten stages each. Both well treatments were recorded, as well as a few days before and afterward.

Site Noise Survey

Initial processing was done with Nanometrics SQLX software. In particular, a PDF database was assembled for PSDs with durations of 1 hour and 10 s. Windows were overlapped by 50%.

Typical results are shown in Figure 4 for array D. Note that the horizontal channels have higher noise levels than the verticals at long periods. This is a typical signature of tilt-induced noise, commonly observed in surface arrays. Above 0.1 Hz, the noise distributions on the horizontal channels are quite similar to that on the vertical channel, and this is the band of interest for the detection of small events anyway, so henceforward we concentrate on the vertical channels.

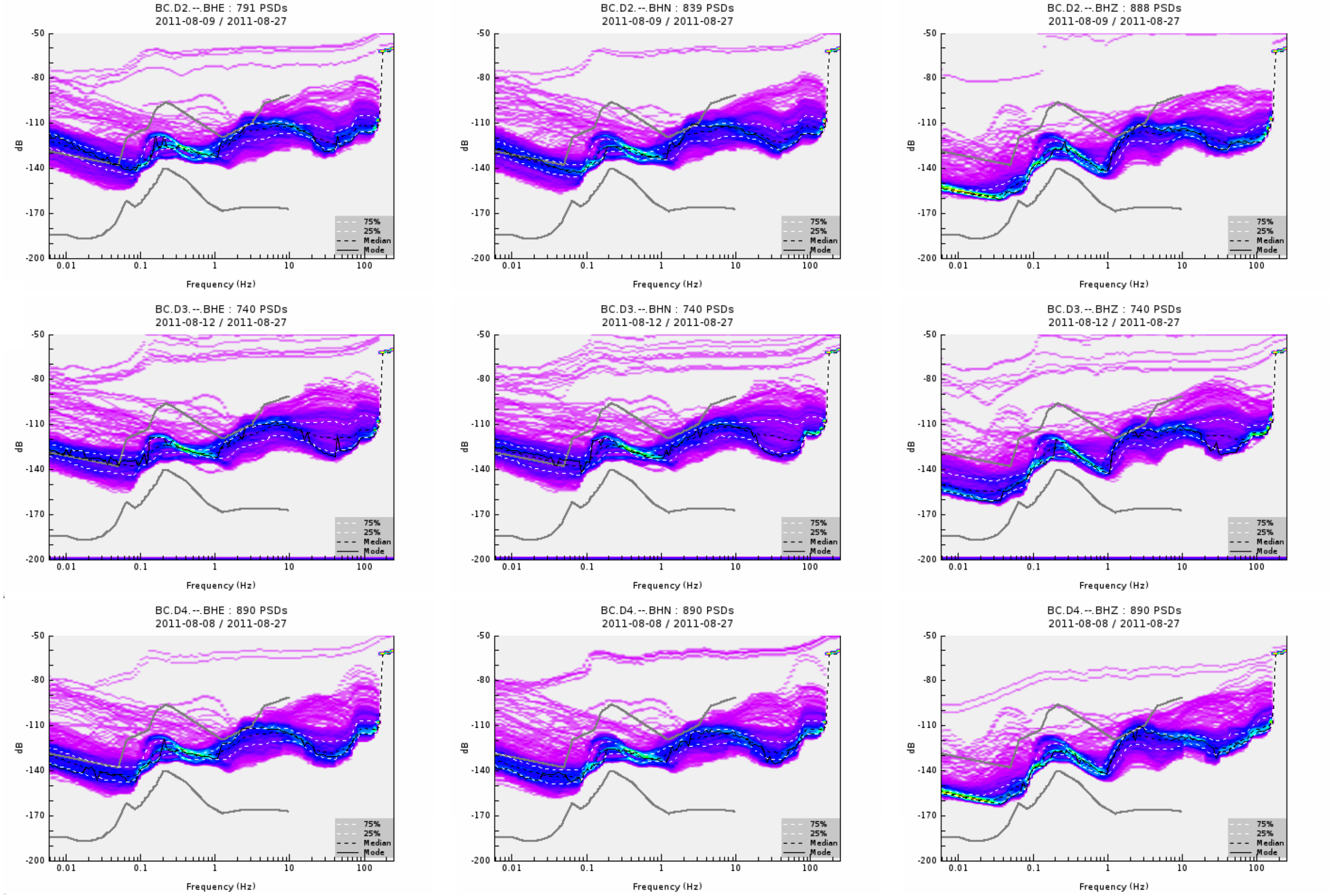

Figure 4: Probability Density Functions at Array D

The noise at the microseismic peak between 0.1 and 1 Hz is bi- or tri-modal. Figure 5 shows PDFs and spectrograms for three vertical channels covering the duration of the experiment. The microseismic peak is not varying on a diurnal schedule but is driven by mid-ocean storms lasting on the order of days. Higher-frequency noise in the band from 1 to 100 Hz has a strong diurnal signature, however.

The horizontal axis of the spectrogram is in Julian days from the start of 2011; the first treatment, for example, was in ten stages starting at the end of day 226 and continuing to the end of day 229. Clearly the diurnal variation is greater than the increase in noise during injection. A pre-frack survey is therefore capable of characterising the site noise for the duration of the hydraulic fracturing.

Although it is beyond the scope of the current presentation, SQLX allows outliers in the PDF to be viewed in the time and frequency domains, and in this case the high-noise outliers were all found to be associated with the initial installation.

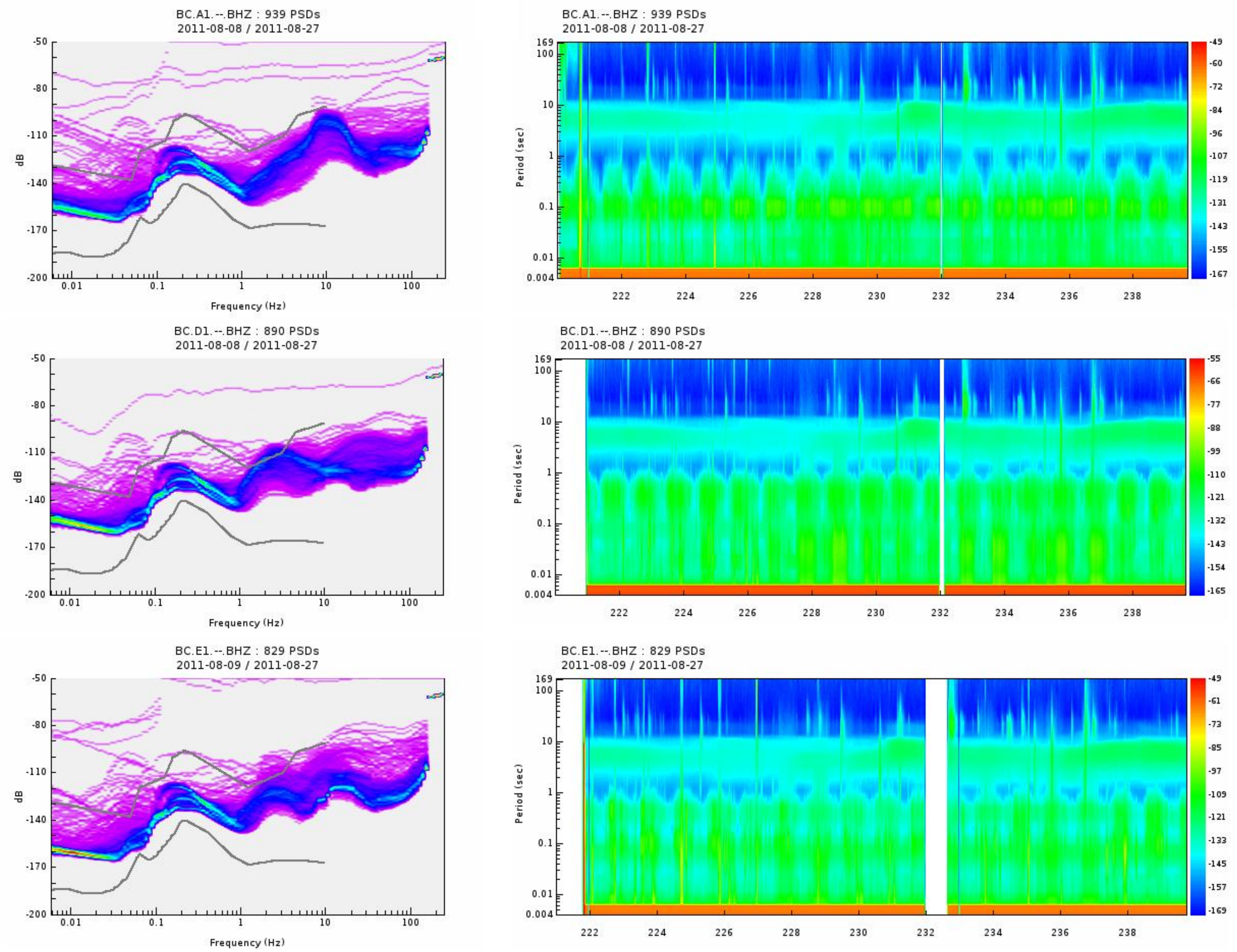

Figure 5: PDF and Spectrogram Signatures at A1, D1 and E1

Figure 5 also shows that above 1 Hz each location has its own noise signature. Site A1 has a large noise peak at 10 Hz, site D1 has a smaller peak at 2.5 Hz, while site E1 has two strong peaks, one at 2.5 Hz and another at 15 Hz.

Since the site noise is roughly constant before, during and after hydraulic fracturing, and yet each site has a distinctive signature, how can the site noise best be characterised for the purpose of assigning limits of detectability? The mode of the PDF tends to be too jagged where the distribution is bimodal; the median gives just a bit too much weight to outliers which usually consist of transients. We chose to use the 25th percentile noise, as being representative of what a given site looks like on a good day, but not the best day.

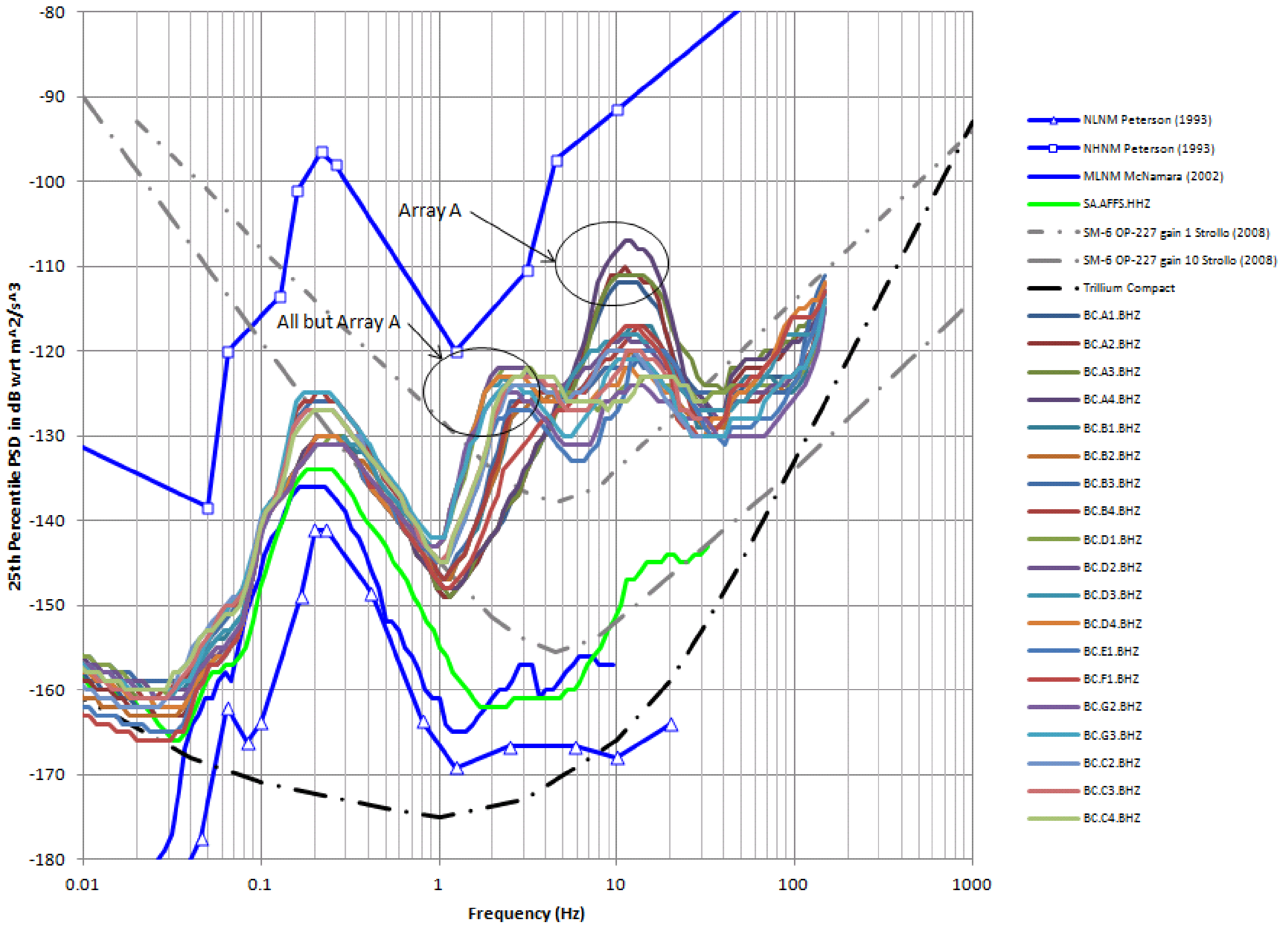

Figure 6: 25th Percentile Vertical Acceleration PSD

Figure 6 shows the 25th percentile vertical ground motion for all stations in the network. Array A shows 10 dB higher noise at 10 Hz than any other station, and it does not show any noise peak near 2.5 Hz band. It is clearly a poor location for monitoring sub-array.

For comparison a 25th percentile vertical ground motion curve from a good site in Saudi Arabia has also included. This is to emphasize that the noise at Rolla in general was particularly high.

For this network, the event detection limit is set not by the sensor used but by the site noise. Having said that, these sites all share a feature which is apparent even in the NHNM and that is a “notch” in the site noise at 1 Hz. In this band at least, a geophone will reduce the signal-to-noise ratio while a broadband seismometer in the class of a Trillium Compact will not.

Aside from correcting the installations of individual sensors, and relocating sub-arrays on the surface, one way to reduce site noise is to install sensors below the surface.

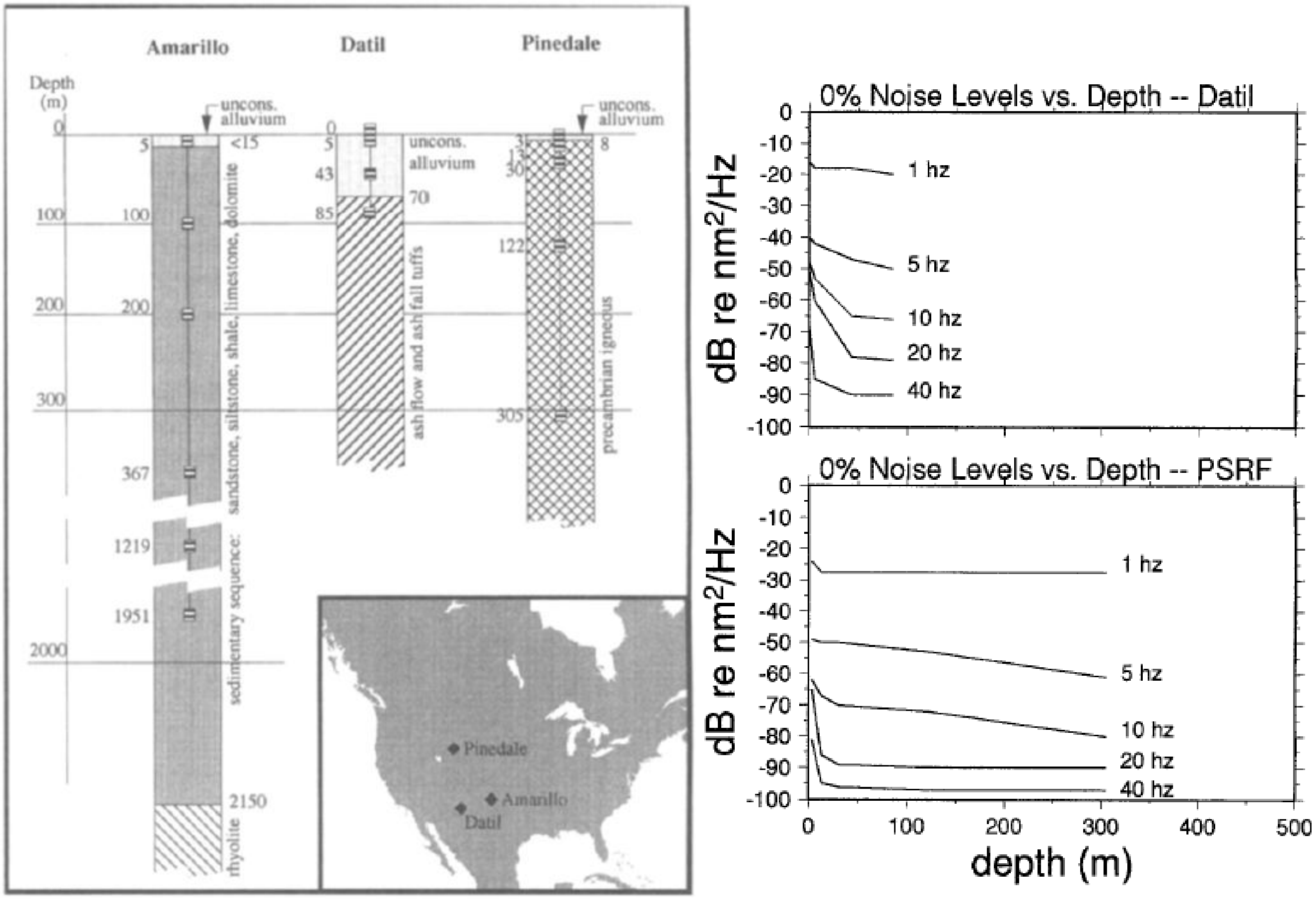

Figure 7: Effect of Depth on Site Noise at High Frequencies

Reprinted from Young et. al. (1996), Figures 1 (left) and Figure 7 (right). The original caption of Figure 1 read: "Stratigraphic columns for each site showing lithology and instrument recording depths. Numbers to the left of columns are recording depths (meters); numbers to the right are lithologic boundary depths. The inset shows the site locations." The original caption of Figure 7 read, in part "Zero percent summary plots of noise level versus depth for selected frequencies …"

The work of Young et. al. (1996) suggests rapid attenuation at high frequency with depth, near the surface. In some cases, most of the improvement happens within the first 10-30 m.

Another way to reduce the site noise is by using array methods. A demonstration of simple stacking is shown in Figure 8.

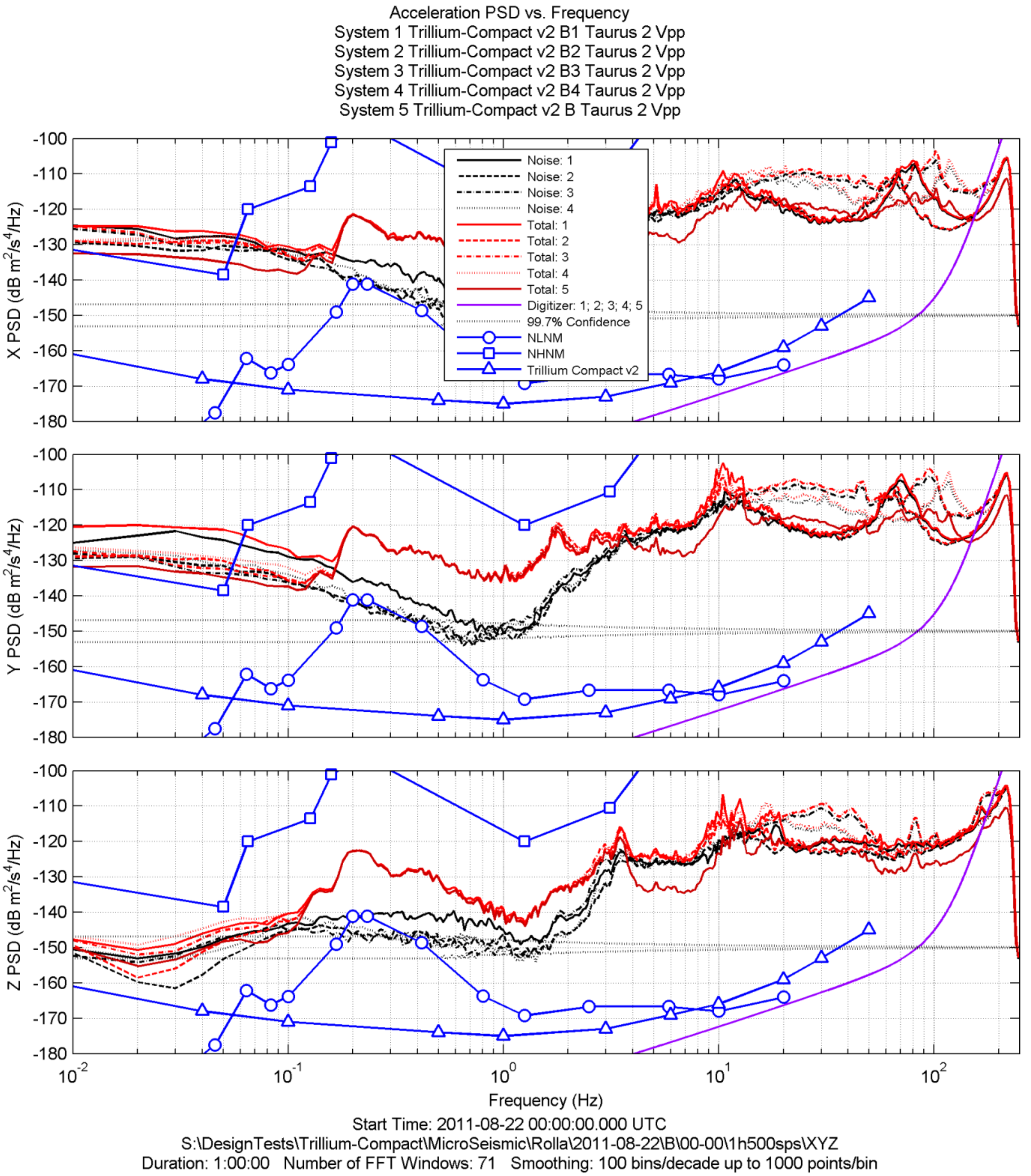
Acceleration PSD vs. Frequency
System 1 Trillium-Compact v2 B1 Taurus 2 Vpp
System 2 Trillium-Compact v2 B2 Taurus 2 Vpp
System 3 Trillium-Compact v2 B3 Taurus 2 Vpp
System 4 Trillium-Compact v2 B4 Taurus 2 Vpp
System 5 Trillium-Compact v2 B Taurus 2 Vpp

Start Time: 2011-08-22 00:00:00.000 UTC
S:\DesignTests\Trillium-Compact\MicroSeismic\Rolla\2011-08-22\B\00-00\1h500sps\XYZ
Duration: 1:00:00 Number of FFT Windows: 71 Smoothing: 100 bins/decade up to 1000 points/bin

Figure 8: Effect of Stacking at Array B

The spectra in Figure 8 were computed using a different tool. The red curves are the PSDs of each of the stations in array B, labeled B1 through B4, plus a stacked result, labeled simply B, produced by simple averaging. The black curves give the non-coherent noise of each of the individual stations, and show that the site noise is coherent across the array up to about 40 Hz. The blue curves are the same NLNM, NHNM and Trillium Compact noise floor used in previous frequency-domain figures.

There are 3 cases of interest:

1. In bands where the signals are coherent, e.g. around the microseismic peak, the stacked signal is no different from that of the individual stations. Because the signals are coherent in this band, this band is useful for misalignment and timing correction. The noise floor of a geophone, regardless of the type of preamplifier used, would be too high for a coherent signal to be measured and allow such corrections.
2. In bands where the signals are non-coherent and near the same level, e.g. 4-8 Hz, there is about 8 dB of improvement. That is to say that the improvement is better than $\sqrt{n}$, where n is the number of stations, which one would expect from simple averaging of noise.
3. In bands where the signals are non-coherent but one or more sensors is much noisier than the others, e.g. 20-50 Hz, the stacked signal is much quieter than the noisiest signal but not necessarily quieter than the quietest signal. To make stacking work in this band, a weighted average would need to be used so that sensors which stood out as being noisier could be de-emphasised in the stacked result.

Because we're stacking by simple averaging, that should be suppressing *surface* noise with half-wavelength equal to the station spacing. Using delay-and-stack methods it should be possible to adjust the array for a different back-azimuth and slowness.

Although the crudest possible method of stacking was used, significant improvement was obtained in a useful band of frequencies, by almost half a unit of earthquake magnitude.

Broadband recordings of regional and teleseismic events which occur during a pre-injection survey can help to explain signals which would otherwise appear anomalous. Figure 9 shows an interesting small event which was found in the Rolla dataset.

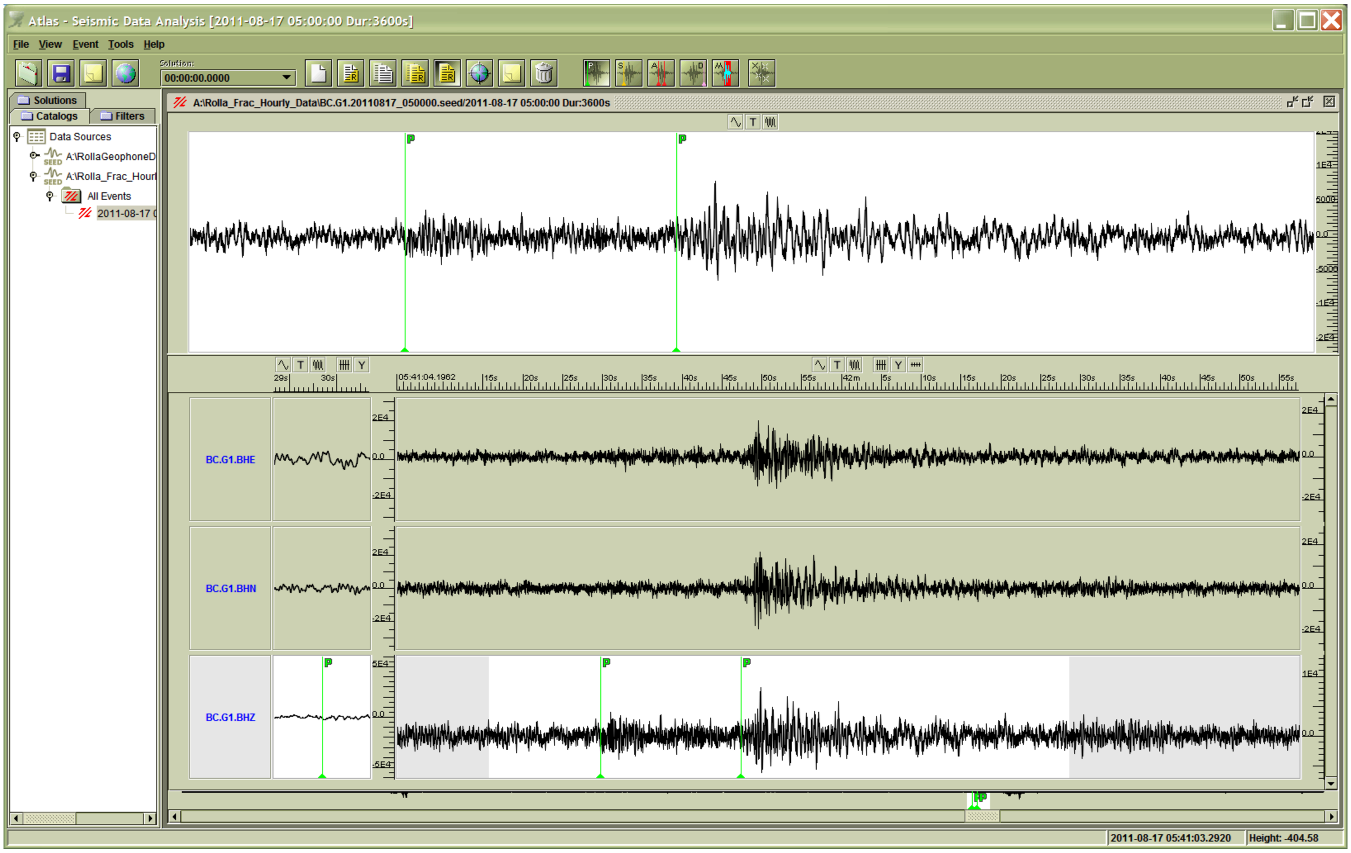

Figure 9: Detected Event

It was initially observed in data from geophones thought to be an LPLD event, of the type discussed by Das and Zoback (2010). Upon examination of the same time period in the broadband data, clear P- and

S-wave arrivals were observed at approximately at approximately 5:41:31 and 5:41:49. Assuming a P- to S-wave velocity difference of 2 km/s this suggests an epicentral distance on the order of 36 km, clearly well outside the area stimulated by hydraulic fracturing. In Figure 9 the data has been band-passed from 0.5 Hz to 8 Hz; on the output of a geophone would not show the S-wave so clearly. The broadband data thus provides a useful reality-check; the event is not an LPLD event.

Conclusions

The noise environment at Rolla varied considerably from array to array and from station to station. The noise environment for any given station remained reasonably static within the band of study for the duration of the deployment. We see very little change in the noise environment before, during and after hydraulic fracturing in the band from 20 s to 100 Hz.

Advanced stacking techniques and sub-surface/near surface installations will help to improve signal to noise ratios, however noisy sites will still impact data processing. It is recommended therefore that whenever possible, sensors be buried as deeply as possible, not to reduce hypocentral distances, but to reduce the impact of surface noise.

Pre-fracturing noise surveys provide valuable information on:

- Where to best situate sensors for best signal-to-noise ratios
- Which sites need something corrected in their installation
- Optimum numbers of stations needed to achieve a given minimum detectable event

Broadband triaxial seismometers allow misalignment and timing corrections by coherently resolving the microseismic peak. They furthermore provide clearer pictures of events which would otherwise appear anomalous.

Acknowledgements

Members and sponsors of the Microseismic Industry Consortium are sincerely thanked for their support. Special thanks are due to David Eaton of the University of Calgary, Sarah Cutten of ARC Industries for providing data and encouragement. Finally, the authors with to thank Kristian Spriggs and Marian Jusko of Nanometrics, Inc. for their hard work in the field.

References

Brune, J. (1970) Tectonic Stress and the Spectra of Seismic Shear Waves from Earthquakes, J. Geophys. Res., Vol. 75, No. 26, pp. 4997-5009.

Peterson, J. (1993) *Observations and modelling of background seismic noise*. Open-file report 93-322, U. S. Geological Survey, Albuquerque, New Mexico.

Young, C., E. Chael, M. Withers, and R. Aster (1996) *A comparison of the high-frequency surface and subsurface noise environment at three sites in the United States*, Bull. Seism. Soc. Am., Vol. 86, No. 5, pp. 1516-1528.

McNamara, D. and Buland, R. (2004) *Ambient Noise Levels in the Continental United States*, Bull. Seism. Soc. Am., Vol. 94, No. 4, pp. 1517-1527.

Strollo, A., S. Parolai, K.-H. Jäckel, S. Marzorati, and D. Bindi (2008) *Suitability of Short-Period Sensors for Retrieving Reliable H/V Peaks for Frequencies Less Than 1 Hz*, Bull. Seism. Soc. Am., Vol. 98, No. 2, pp. 671-681.

Fisher, M.K. (2010) *Data Confirm Safety of Well Fracturing*. American Oil and Gas Reporter. July.

Das, I., and Zoback, M. (2011) *Long-period, long-duration seismic events during hydraulic fracture stimulation of a shale gas reservoir*: The Leading Edge, Vol. 30, No. 7, pp. 778–786.

Ackerley, N. (2012) *Estimating the Spectra of small events*, Poster Presentation, GeoConvention 2012, forthcoming.